Relationship between deformation, plutonism and regional metamorphism in the Markstein area (southern Vosges)*

Katja PETRINI (1)
Jean-Pierre BURG (1)

Relations entre déformation, plutonisme et métamorphisme régional dans la région de Markstein (Vosges du Sud)

Géologie de la France, n°2, 1998, pp. 13-23, 6 fig.

Key words: Turbidites, Upper Devonian, Visean, Granites, Regional metamorphism, Contact metamorphism, Folds, Hercynian Orogeny (Vosges Mountains).

Mots-clés : Turbidites, Devonien supérieur, Viséen, Granites, Métamorphisme régional, Métamorphisme contact, Pli, Orogénie hercynienne, Massif vosgien.

Abstract

The Markstein formation (southern Vosges) consists of turbiditic sequences and pebbly mudstones deposited at the extremity of a delta fan and/or on the proximal part of a continental slope. The area has been affected by regional deformation responsible for open to tight folds trending N130° with an associated axial-plane cleavage. During deformation, a regional metamorphic event in places reached the biotite isograd in metapelites.

The Markstein sediments were intruded ca. 340 Ma ago by shoshonitic-type granites that produced a contact metamorphism expressed by spotted (cordierite) slates and hornfels. An associated deformation, resulting mainly in the formation of a cleavage, is limited to a narrow aureole (<200 m) around the plutons. The cordierite crystallization was contemporaneous with or shortly followed the regional metamorphism and deformation, indicating that the regional and the contact-related events were sub-contemporaneous. Hence, the age of the plutons constrains the age of the regional deformation, which would have taken place shortly before 340 Ma ago (Late Visean).

Résumé

La formation du Markstein, située dans l'avant-pays varisque des Vosges du Sud, est constituée de séries turbiditiques dans lesquelles s'intercalent des coulées boueuses à galets. Les structures sédimentaires et la distribution des sédiments suggèrent un dépôt en front de delta et (ou sur) la partie proximale du talus continental. La déformation régionale est responsable de la formation de plis serrés d'axes orientés N130°E en moyenne. A ce plissement, sont associés une schistosité de plan axial et un métamorphisme atteignant dans les métapélites l'isograde de la biotite. Des granites de composition shoshonitique ont intrudé ces sédiments, il y a environ 340 Ma. Ils ont engendré un métamorphisme de contact à l'origine de cornéennes aux bordures des granites et de schistes tachetés (de cordiérite) jusqu'à 1500 m des contacts intrusifs. Le magmatisme est associé à des déformations localisées et, en particulier, à la formation d'une schistosité sur une distance inférieure à 200 m de la bordure des plutons. Nous montrons que la déformation régionale et le magmatisme sont péné-contemporains, et donc que l'histoire tectono-métamorphique de la région du Markstein est d'âge Viséen supérieur.

Introduction

The aim of this study is to document the relationship between regional deformation and plutonism in the regionally low-grade foreland of the Variscan southern Vosges (Fig. 1). Previous geological work in the Markstein area has covered sedimentology (Gagny, 1963; Gagny, 1964; Grimm, 1983; Schneider, 1990) as well as petrography and geochemistry of the plutonic rocks (Gagny, 1968; Langer *et al.*, 1995), but no detailed investigation of the structures and metamorphic crystallization and their relationship.

We first describe the sediments that underlie most of the area and we refer largely to Gagny's work (1968) for a description of the granites. We then present our observations on the metamorphism and the structures, systematically distinguishing between regional and contact features. We also discuss the relationship

* Manuscrit déposé le 10 février 1998, accepté le 17 juillet 1998.
(1) Institute of Geology, Department of Earth Sciences, ETH-Zentrum, Sonneggstr.5, 8092 Zurich, Switzerland.

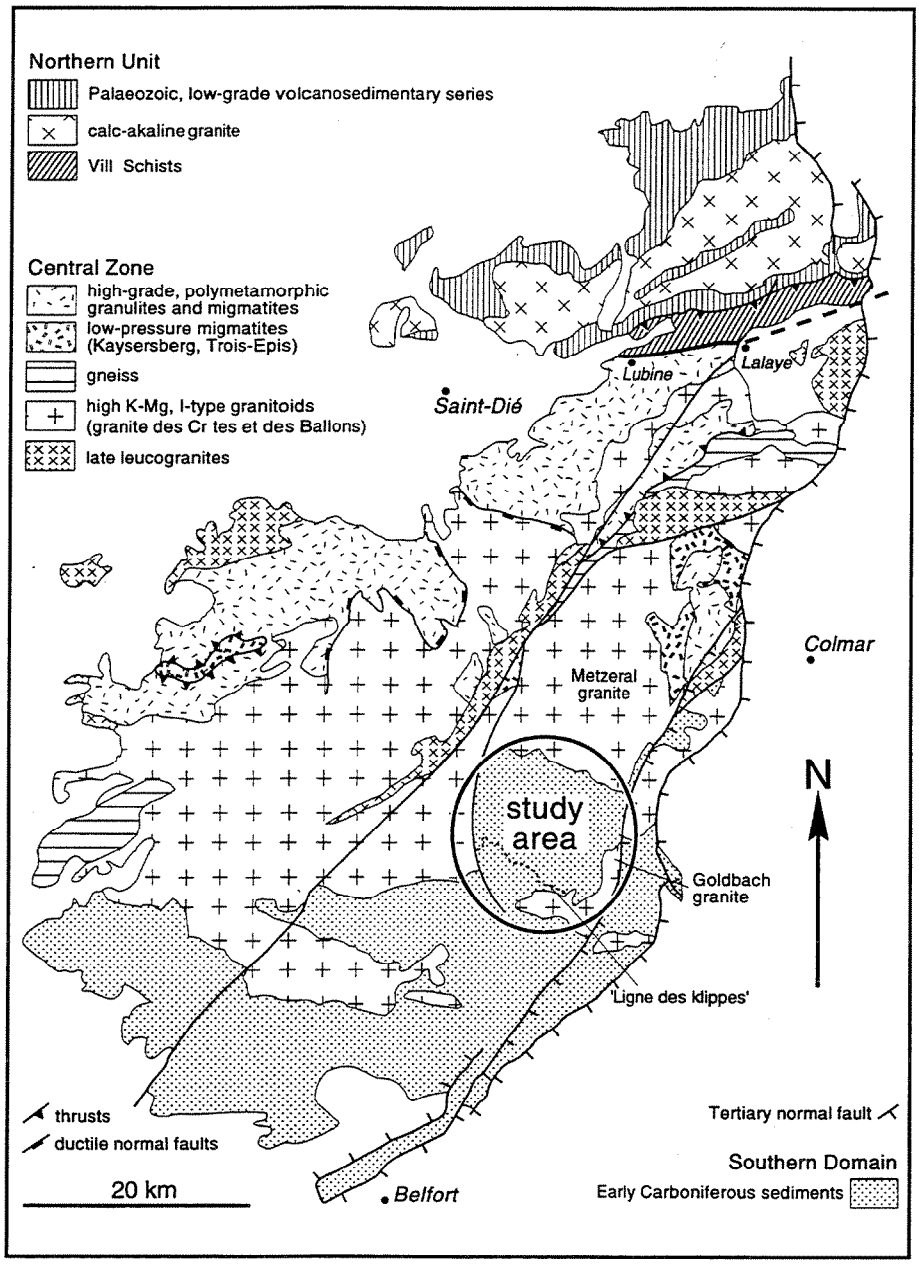

Fig. 1.- Simplified geological map of the Vosges (modified after Fluck *et al.*, 1989), showing the location of the study area (circled).

Fig. 1.- Carte géologique simplifiée du socle vosgien (modifiée d'après Fluck et al., *1989) et localisation de la région étudiée (encerclée).*

between deformation and contact metamorphism. Finally, we argue that the plutonism was subcontemporaneous with the regional deformation and metamorphism.

Geological setting

The studied area is located in the "Moldanubian zone" of the southern Vosges massif (Kossmat, 1927), which consists of Upper Devonian to Lower Carboniferous (Dinantian) sedimentary sequences. The division of the southern Vosges into lithostratigraphic units is disputed, with a "French school" (e.g. Fourquin, 1973; Coulon, 1975) presenting ideas partly contrasting with those of a "German school" (e.g. Grimm, 1983; Maas, 1988). According to the French school, the Markstein formation is an allochthonous unit separated from contemporaneous units located farther to the south by a "tectonic line" called the "Ligne des Klippes", whereas the German school considers the Markstein unit to be in continuity with, and a distal equivalent of, the units located to the south with all the sedimentary units representing sedimentation in a single basin. Moreover, deformation in the Markstein occurred during the late Visean according to the French authors and during the Stephanian according to the Germans.

Sediments of the Markstein formation

The Markstein area is characterized by an association of Upper Devonian to late Visean greywacke and siltstone/pelite organized into turbiditic sequences (Gagny, 1963) – i.e. beds of greywacke, a few centimetres to several metres thick, alternating with minor siltstones and pelites. At places, pebbly mudstones with well-rounded pebbles of various sizes and lithologies (Grimm, 1983), and locally with diameters of a few decimetres (Fig. 2a), attest to multiple catastrophic mudflows.

Greywackes

The average grain size of the greywackes is 2 mm in the coarse layers and 4 μm in the finer layers. Sorting, especially in the coarse layers, and degree of rounding are poor. Numerous sedimentary structures such as grading, load marks and cross bedding can be observed. Mineralogically the greywackes are characterized by 40 to 70% feldspar (zoned plagioclase with 20 to 40% anorthite content and orthoclase showing microcline-like twins), 5 to 35% quartz and lithic fragments (granite, granitoid, quartz porphyry, greywacke and, in the southern part of the studied area, volcanoclasts). The matrix (10% to 20% vol.) consists of clay cement that has been silicified and recrystallized, probably during diagenesis. Accessory minerals include amphibole, apatite, zircon, epidote and some opaques.

Siltstones/pelites

The siltstones and pelites are finely layered rocks displaying many macroscopic and microscopic sedimentary structures, such as ripples and cross bedding, and microscopic syn-sedimentary normal faults. Qualitatively, the main constituents are fine-grained biotite and chlorite. The amount of quartz with respect to feldspar

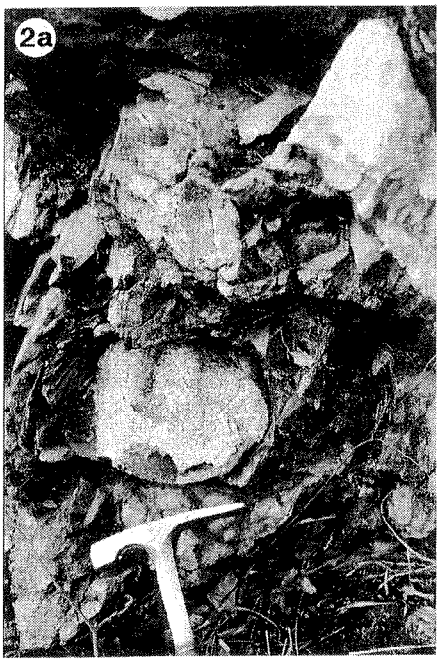

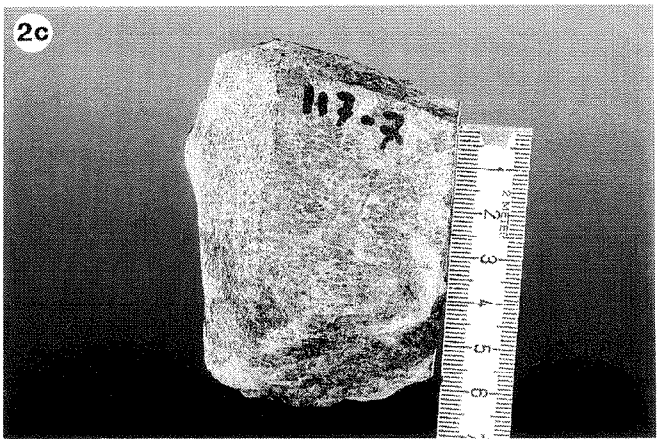

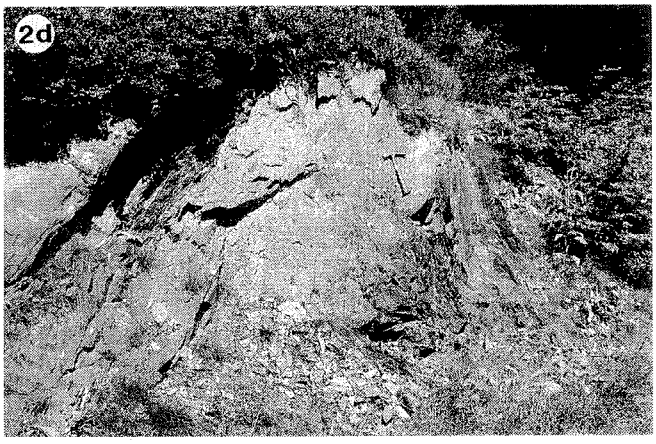

Fig. 2.- a) Pebbly mudstone with a large granitic pebble, Chemin de l'Eibel, East of Col du Plaezerwaesel (coordinates: 7°2'51"E, 47°58'5"N).
b) Complete ('Bouma') turdibitic sequence, Chemin de l'Eibel; bed dips toward the SW.
c) Spotted slate from the proximity of the Metzeral granite, at Brobachrucken (coordinates 7°5'28"E, 47°59'52"N).
d) Fold hinge (fold axis trends 015°/plunge 10°). Route des Crêtes (7°3'52"E, 47°54'42"N).

Fig. 2.- a) Ecoulement boueux conglomératique à galet granitique, Chemin de l'Eibel, Est du col du Plaezerwaesel (coordonnées: 7°2'51"E, 47°58'5"N).
b) Séquence turbiditique complète ('Bouma'), Chemin de l'Eibel ; pendage des couches vers le sud-ouest.
c) Schistes tachetés situés à proximité du granite de Metzeral, à Brobachrucken (coordonnées 7°5'28"E 47°59'52"N).
d) Charnière de plis (axe de plis 015°/10°). Route des Crêtes (7°3'52"E, 47°54'42"N).

is greater than in the greywackes. Some pelites contain up to 5% opaques.

Sedimentary environment and source

The turbidite units consist of coarse-grained greywacke overlain by finer grained layers. Bottom boundaries are slightly erosive. The coarse basal term consists of sequences of amalgamated turbidites, as indicated by grading and pebbles of pelitic layers within the greywackes. The upper finer layers consist of alternating fine-grained greywacke and pelite constituting fining-upward sequences.

The alternation of greywacke and pelite is irregular but, as a general observation, the sequences tend to be thicker and clearly dominated by greywacke in the southern part of the studied area, whereas the sand/clay ratio decreases to the north where alternations are thinner and complete turbiditic sequences (Bouma, 1962) are observed (Fig. 2b). This distribution and the bulk grain-size decreasing northwards suggest sedimentary input from the south. The average paleoflow direction measured during this study from ripples, flow-marks and imbricated grains is towards N070°, in accordance with measurements reported by B. Grimm (1979). Moreover, outcropping equivalents of the pebbles are found exclusively to the south of the studied area (Grimm, 1983). Therefore, the source area was located to the south or southwest of the Markstein area. The low anorthite content and primary zoning of the feldspar clasts suggest that these have a magmatic origin, and the presence of microcline implies a plutonic source.

The immaturity of the greywackes (especially the high content of feldspars), the poor sorting and the poor degree of rounding suggest a relatively short transport distance. The abundant clastic material and the amalgamations are consistent with a proximal character, along with remains of channels. It is therefore likely that the Markstein formation was located in a distal part of a delta fan and in the proximal part of a slope.

Granitoids

The sediments in the mapped area lie between two main plutons: the Metzeral granite to the north and west and the Goldbach granite to the south and east (Fig. 1). The contacts between the sediments and both plutons are poorly exposed: the contact between the Markstein formation and the Metzeral granite is intrusive in places, although more generally faulted, and the contact with the Goldbach granite is faulted, but at few places (see also the Munster sheet of the 1:50,000-scale Geological map of France). The mineralogy of the granites is dominated by K-feldspar (orthoclase and microcline) and quartz, with minor amphibole (Mg-actinolite), biotite and plagioclase. Accessory minerals include apatite, pyrite, zircon, sphene and allanite. Based on a study of their average chemical composition (Gagny, 1968), the alkali/silica ratio indicates a transitional composition between alkaline and subalkaline. The high potassium content points to a shoshonitic character, typical for magmas emplaced during the mature stages of orogeny in a continental plate (D'Amico *et al.*, 1987).

The Metzeral granite is dated at 341 ± 1 Ma (U-Pb on zircons, Schaltegger, 1995). Biotite of the "granites des Crêtes" yields an Ar-Ar age of 333 ±1 Ma (Boutin *et al.*, 1995).

Metamorphism

Study of the metamorphism in the Markstein sediments is hindered by pervasive weathering and the very small size of the metamorphic crystals (*ca.* 15 μm). Consequently, precise pressure-temperature determination was impossible. Nevertheless, various stages can be inferred and some reactions can be suggested for the regional and contact metamorphism. It will be shown that the regional and contact metamorphic peaks succeeded each other in a short time interval.

Regional low-grade metamorphism

The principal variable in the regional metamorphism is the rock composition: at the same place different mineral parageneses are found in different rock types, and rocks of similar characteristics (e.g. bulk composition, grain size, etc.) have the same mineral assemblages, except near the plutons (<1500 m). The following regional parageneses have been detected:

- in the greywackes: quartz - phengitic muscovite – chlorite;

- in the pelites and siltstones: quartz - biotite - phengitic muscovite – chlorite.

Both mineral associations characterize a low-grade metamorphism.

Petrographic and textural observation suggests that the pelite/siltstone assemblage formed by the continuous simplified reaction (Mather, 1970):

phengitic muscovite + chlorite → less phengitic muscovite + chlorite + biotite + H_2O.

Due to the very fine size of the micas and to their poor crystallization, which produced interlaminations, microprobe analyses were not able to provide evidence for a decrease in the FeO and MgO content of the muscovite as the reaction proceeded. The distribution coefficients for FeO and MgO in micas appearing together are variable and nowhere equal 1 (cf. appendix), which suggests that the above reaction did not reach an advanced stage. It is known that this reaction is critically dependent on chemical variables such as Al-content (Atherton, 1968) or Fe-Mg ratio (Spear, 1993). Thus minor changes in the composition of the system may have led to different stages of this reaction being reached, resulting in different mineral assemblages. This would explain that biotite has been reported in greywackes but not in pelites (Mather, 1970). Since no evidence of a retrograde reaction was found, we conclude that the whole region just reached the biotite isograd.

Contact metamorphism

Contact metamorphism is responsible for higher temperature mineral assemblages in a *ca.* 1500 m wide aureole around the plutons. Two zones can be distinguished: an inner aureole of proper hornfels and an outer aureole of spotted slates (Fig. 2c).

The hornfels zone is usually restricted to 75-100 m from the contact. The rocks are typically dark, completely recrystallized and massive. Microscopically, they show typical decussate textures with a

quartz - biotite - chlorite mineral assemblage. By plotting the electron microprobe analyses (see appendix) on an Al_2O_3-$KAlO_2$-FeO+MgO ternary diagram together with the bulk rock composition, it becomes obvious that a K-bearing phase is present. This unidentified phase is probably a very fine (<5 μm) white mica (muscovite or phengite), which will be considered as present in the following discussion.

The spotted aspect of the outer aureole slates (Fig. 2c) is due to cordierite blasts, generally altered to pinite although a few relatively fresh cordierite crystals have been identified by their characteristic twinning. Electron microprobe analyses (see appendix) show that, compared to fresh cordierite, the altered blasts are richer in K and in Al and depleted in Fe and Mg. Flakes of white mica (muscovite-phengite), biotite and chlorite have been identified within the spots. In addition to the cordierite spots, the rock matrix is characterized by a white mica-biotite-chlorite assemblage. Since biotite and chlorite are intimately associated, especially far from the contact, it is difficult to obtain a single phase analysis.

Our mapping suggests the following distribution:

(1) a background regional assemblage comprising quartz - phengitic muscovite - biotite – chlorite;

(2) appearance of cordierite at *ca.* 1500 m from the pluton borders as part of the assemblage quartz - phengitic muscovite - biotite (interlayered with chlorite) – cordierite;

(3) disappearance of chlorite on approaching the contact (<150 m) to give an assemblage of quartz - phengitic muscovite - biotite – cordierite; finally

(4) cordierite disappears in the immediate proximity (few metres) of the contact, leaving the assemblage as quartz – muscovite (inferred) - biotite - chlorite.

The interlamination of chlorite and biotite and the presence of muscovite and chlorite within the spots support the following reaction for the crystallization of cordierite in (2):

muscovite + chlorite + quartz → cordierite + biotite + H_2O (Yardley, 1989).

Approaching the pluton, as the reaction proceeded, muscovite disappears and excess chlorite is left in very small amounts. In (4) the absence of cordierite is attributed to retrograde metamorphism possibly caused by a limited release of water during cooling of the pluton. The reaction generating cordierite may also account for its destruction, resulting in a paragenesis that is the same as the background assemblage (quartz - muscovite - biotite - chlorite).

Deformation in the Markstein formation

Regional folding

Folding is expressed throughout the studied area by fold hinges (Fig. 2d) and by the steep dips of bedding and cleavage in limb areas (Fig. 3). Fold axes in the centre of the studied area trend N130° and plunge 10° to 30° in either direction (Fig. 4); close to the plutons, fold axes vary in orientation (see below). The folding style is heterogeneous with large variations of interlimb angles. Deformation in the pelitic and greywacke layers is decoupled and results in disharmonic folds.

Fold hinges were found only along bands oriented parallel to the large regional fold axes. We interpret these bands as the trace of major hinge zones. Three major antiforms and two major synforms with wavelengths of a few kilometres are constructed (Fig. 5). Folds recorded in the outcrops are consistently parasitic folds related to these larger synforms and antiforms. Folding accounts for *ca.* 50% shortening of the sedimentary formation. Due to folding, the rocks have developed an axial-plane cleavage locally difficult to detect. In the coarser grained layers, the cleavage may be represented by fractures.

Contact-related deformation

The most obvious feature related to the contact aureole is the development of a penetrative cleavage, apparently more intense than the axial-plane cleavage observed regionally. It is marked by the preferred orientation of phyllosilicate and cordierite blasts. Attempts to quantify strain changes were performed through X-ray diffraction texture goniometry, but failed partly because of the strong primary anisotropic character of the initial sediments and partly because of the presence of porphyroblasts affecting the orientation of mica flakes in their vicinity.

Open, sub-horizontal buckle folds are observed close to the intrusion. These folds trend mainly N-S; they are distinctly different from the regional folds, with more regular amplitudes (20-30 cm) and wavelengths (50 cm). No axial-plane cleavage has been observed in these folds.

Relationship between regional and contact deformation

The scarcity of rock exposure hampers an extensive and definitive structural geology study of the area. The orientation of the fold axes varies close to the plutons (Fig. 4) where folds are no tighter than in the central area. This variation in orientation may represent an interference between regional and pluton-related deformation, but it does not show a consistent pattern and no superposition has been observed. The study of cleavages is more conclusive in interpreting the relationship between the two deformations. Despite considerable effort, no superimposition of the contact-related cleavage with the regional axial-plane cleavage has been observed on either a macroscopic or microscopic scale. Contact-related cleavage coincides with an absence of regional cleavage and vice versa. This observation suggests a nearly coeval development of the regional and the aureole foliations.

Discussion

A time-related occurrence of regional events and plutonism may be inferred from both petrologic and structural observations. Regional folding and metamorphism seem to be in continuity with pluton-related events. The appearance of cordierite, according to the previously described reaction and conditions, is expected to occur at *ca.* 520 °C. A simple thermal calculation shows that the plutons alone could not

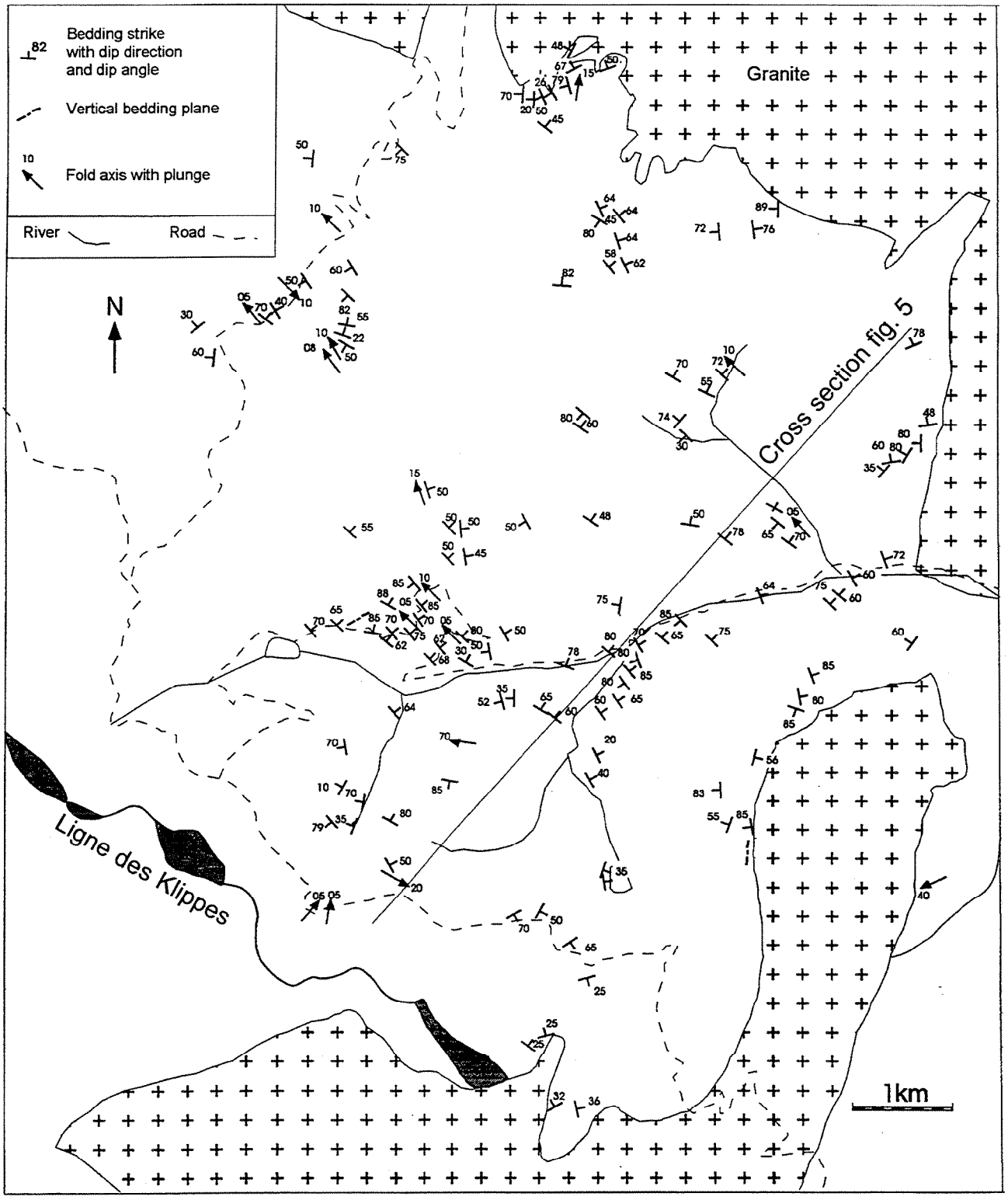

Fig. 3.- Structure orientations in the Markstein formation and line of the cross section in Figure 5.

Fig. 3.- Orientations structurales dans la série du Markstein et tracé de la coupe de la figure 5.

have provided the energy sufficient to generate this temperature.

The model applies to a conduction of heat for an instantaneous spherical source body as described by Carslaw and Jaeger (1959) and does not take into account the effects of latent heat from solidification and convection after emplacement. Necessary parameters for the calculation are the diameter of the pluton, its emplacement temperature and the initial temperature of the country rocks. The diameter of the Metzeral pluton is estimated at about 8 km, and the diameter of the Goldbach pluton at about 2.5 km (Munster sheet of the 1:50,000-scale Geological map of France). The

emplacement depth of the plutons is 3 to 4 km (Gagny, 1968; Grimm, 1983). A normal to high geothermal gradient of 25 °C/km accounts for an initial sediment temperature at this depth of 100 °C. The solidus temperature for a magma with the relevant chemical composition, assuming it is water saturated, is between 650 and 700 °C (Tuttle and Bowen, 1958; Wyllie, 1977). Calculations (Fig. 6) show that, for both granites, the temperature in the sediments (even within 100 m of the contact) should not exceed 400 °C. Various factors (advecting fluids, slow emplacement, etc.) can affect the shape of the temperature-time lines (Fig. 6), but would not significantly increase the maximum temperature reached in the proximity of the plutons. The discrepancy between the modelled temperatures (T<400 °C) and the inferred metamorphic reaction occurring at T>520 °C requires some explanation. First, CO_2-rich fluids may stabilize cordierite at lower temperatures. To stabilize cordierite at a temperature of 450 °C the partial pressure of CO_2 must be as high as 0.8, which is unlikely considering the pelitic lithologies involved (Ghent, 1975; Ferry, 1992). Second, the presence of water in its lattice is able to stabilize cordierite at low temperatures (Winkler, 1996). However, these factors alone cannot explain the large difference between the modelled and inferred temperatures.

Increasing the calculated temperatures in the country rocks may be performed by increasing the heat transfer by convection within the pluton. However, given the shallow plutonism, it is likely that magma viscosity was too high for convection to play an important role. The remaining possibility is to consider that the country rock temperature was initially higher than the temperature used for calculation. If the country rocks had an initial temperature between 350 and 400 °C, a temperature >520 °C can be reached over a distance of several hundred metres from the pluton. Initial

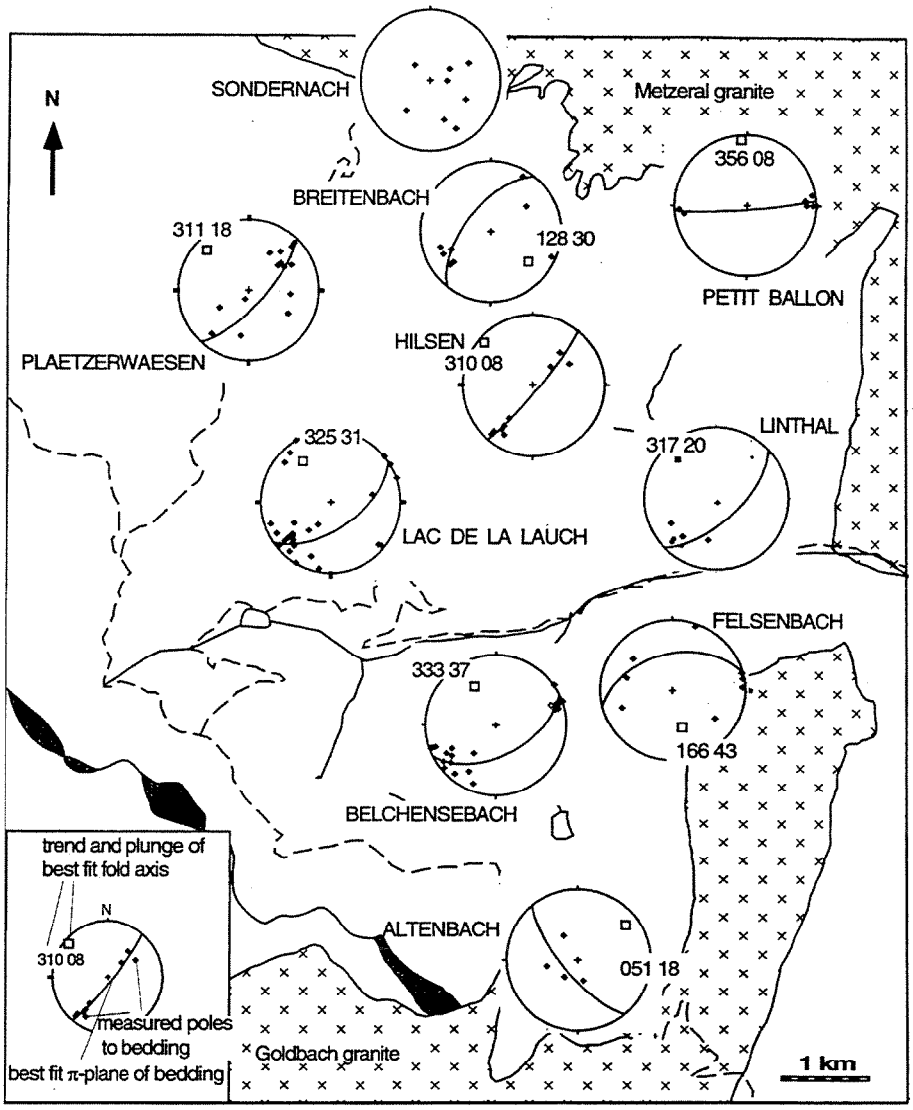

Fig. 4.- Orientation diagrams of poles to bedding planes at different localities throughout the studied area (Schmidt net, lower hemisphere).

Fig. 4.- Diagramme d'orientation des pôles des stratifications en différentes localités (Canevas de Schmidt, hémisphère inférieur).

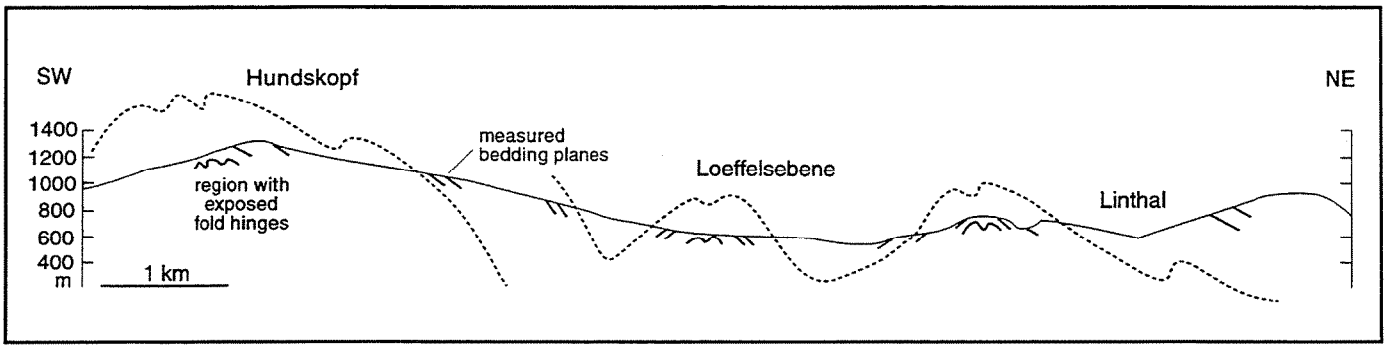

Fig. 5.- Cross section of the studied area (cf. Fig. 3 for location).

Fig. 5.- Coupe interprétative, localisée en figure 3.

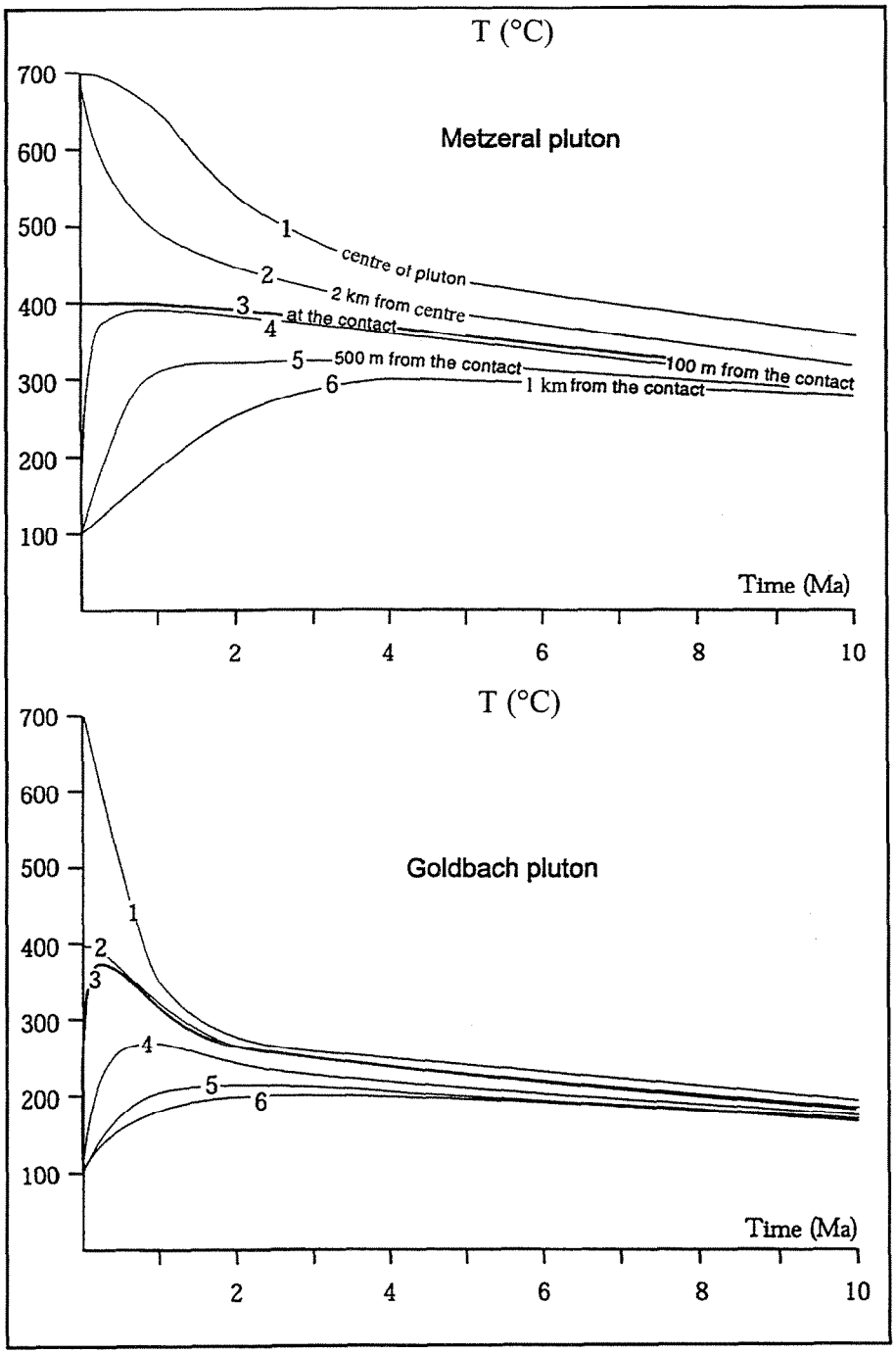

Fig. 6.- Temperature-time curve in the granites and surrounding country rocks.

Fig. 6.- Lignes température-temps pour les granites et leurs encaissants.

temperatures of 350-400 °C correspond to the temperature at which biotite starts to form in greywackes, in agreement with our observation. Therefore, this calculation further suggests that the plutonism was nearly coeval with the regional metamorphism.

Under such circumstances it may be argued that the regional deformation itself was due to plutonism. A few arguments seem, however, to stand against this hypothesis: 1) if the regional folds were generated by the plutons, an increase in the folding intensity would be expected towards the contacts and this is not observed; 2) the fold axes do not show a consistent pattern developing around the plutons, but display a consistent regional trend disturbed by the plutons; and 3) folding accounts for *ca.* 50% shortening in the sedimentary formation, which is too much to be attributed to the intrusion of small plutons over the area considered. Therefore the regional folds are probably not a space-accommodation shortening.

Conclusions

The Markstein area represents a turbidite sequence consisting of greywackes and pelites. The mineralogy and the textural immaturity of the greywackes suggest a relatively short transport distance and deposition at the bottom of a delta fan and the proximal part of a continental slope. Sediment supply was from the southwest.

The sediments were intruded at 341±1 Ma (age of the Metzeral granite, Schaltegger, 1995). The shoshonitic composition of the granites indicates late orogenic intrusions.

There was a close time relationship between the regional folding and plutonism. The age of the intrusions can therefore be used to constrain the age of the regional deformation that should have occurred about 340 Ma ago, shortly after deposition. This conclusion agrees with Boutin *et al.* (1995) who performed K-Ar and ^{39}Ar-^{40}Ar dating on several intrusions and metamorphic rocks throughout the Vosges and determined a minimum age for the metamorphism of 330-340 Ma.

Aknowledgements

Fieldwork was supported by the BRGM. We thank D. Bernoulli and J. C. Maurin for help and discussions in the field.

References

Atherton M. P. (1968) - The variation in garnet, biotite and chlorite composition in medium grade pelitic rocks from the Dalradian, Scotland, with particular reference to the zonation in garnet. *Contrib. Mineral. Petrol.*, **18**, 347-371.

Bouma A. H. (1962) - Sedimentology of some flysch deposits: a graphic approach to facies interpretation. Amsterdam, Elsevier, 168 p.

Boutin R., Montigny R., Thuizat R. (1995) - Chronologie K-Ar et Ar-Ar du métamorphisme et du magmatisme des Vosges. Comparaison avec les massifs varisques avoisinants. *Géologie de la France*, n° 1, 3-25.

Carslaw H. S., Jaeger J. C. (1959) - Conduction of Heat in Solids. Oxford University Press., 510 p.

Coulon M. (1975) - Contribution à la connaissance stratigraphique du Culm des Vosges méridionales. *Ann. Soc. Géol. Nord*, **96**, 4, 387-398.

D'Amico C., Innocenti F., Sassi F. P. (1987) - Magmatismo e metamorfismo. Collezione Scienze della Terra, Torino, Unione Tipografico-Editrice Torino. 536 p.

Ferry J. M. (1992) - Regional metamorphism of the Waits river Formation, Eastern Vermont: delineation of a new type of giant metamorphic hydrothermal system. *J. Petrol.*, **33**, 45-94.

Fluck P., Edel J. B., Gagny C., Montigny R., Piqué A., Schneider J. L., Whitechurch H. (1989) - Carte synthétique et géotraverse N-S de la chaîne varisque des Vosges (France). Synthèse des travaux effectués depuis deux décennies. *C. R. Acad. Sci., Paris*, **309**, 2, 907-912.

Fourquin C. (1973) - Contribution à la connaissance du tectonogène varisque dans les Vosges méridionales. I. Le Culm de la région de Giromagny. *Sci. Géol., Bull.*, **26**, 1, 3-42.

Gagny C. (1963) - Caractères sédimentologiques et pétrographiques des schistes et grauwackes du Culm dans les Vosges méridionales. *Bull. Serv. Carte géol., Alsace Lorraine*, **15**, 4, 139-160.

Gagny C. (1964) - Interprétation des laminites dans une série à turbidites du Culm des Vosges méridionales. *Bull. Soc. géol. Fr.*, **6**, 43-51.

Gagny C. (1968) - Pétrogenèse du granite des Crêtes (Vosges méridionales). Thesis, Université de Nantes, 546 p.

Ghent E. (1975) - Temperature, pressure, and mixed-volatile equilibria attending metamorphism of staurolite-kyanite-bearing assemblages, esplanade Range, British Columbia. *Geol. Soc. Amer. Bull.*, **86**, 1654-1660.

Grimm B. (1979) - Geologische Untersuchungen im Palaeozoikum bei Sondernach (Suedvogesen). Freiburg i.BR., Universitaet Freiburg i. Br., 52 p.

Grimm B. (1983) - Petrographische Untersuchungen an Geroellen des Markstein Bereiches (Palaeozoikum, Suedvogesen). Freiburg i. Br., Universitaet Freiburg i. Br., 80 p.

Kossmat F. (1927) - Gliederung des variszischen Gebirgsbaues. *Abh. Sächs. Geol. Landesamt*, **1**, 1-39.

Langer C., Altherr R., Hegner E., Satir M., and Henjes-Kunst F. (1995) - Moldanubian granitoids of the Vosges: evidence for diverse crustal and mantle sources. *Terra Abstr.*, 7, 1, 299 p.

Maas R. (1988) - Die Südvogesen in variszischer Zeit. *Neues Jb. Geol. Paläontol. Monatsh.*, Stuttgart, **10**, 611-638.

Mather J. D. (1970) - The biotite isograd and the lower greenschist facies in the Dalradian rocks of Scotland. *J. Petrol.*, **11**, 2, 253-275.

Rivalenti G., Sighinolfi G. P. (1969) - Geochemical study of greywackes as a possible starting material of para-amphibolites. *Contrib. Mineral. Petrol.*, **23**, 173-188.

Schaltegger U. (1995) - High-resolution chronometry of Late Variscan extensional magmatism and the basin formation: examples from the Vosges, Black Forest and the alpine basement. *Terra Nostra*, 7, 95, 109-111.

Schneider J. L. (1990) - Enregistrement de la dynamique varisque dans les bassins volcano-sédimentaires dévono-dinantiens: exemple des Vosges du Sud. Strasbourg, Université Louis Pasteur, 205 p.

Spear F. (1993) - Metamorphic phase equilibria and P-T-t paths. *Mineral Soc. Amer. Monogr.*, 799 p.

Tuttle O. F., Bowen N. I. (1958) - Origin of granite in the light of experimental studies in the system $NaAlSi_3O_8$-$KAlSi_3O_8$-SiO_2-H_20. *Geol. Soc. Amer. Mem.*, **74**, 153.

Winkler B. (1996) - The dynamics of H_2O in minerals. *Phys. Chem. Miner.*, **23**, 4-5, 310-318.

Wyllie P. J. (1977) - Crustal anatexis: an experimental review. *Tectonophysics*, **43**, 41-77.

Yardley B. M. D. (1989) - An Introduction to Metamorphic Petrology. New York, Longman. 248 p.

Appendix

WHOLE ROCK COMPOSITION

	fine grained samples			coarse grained samples		
SiO2	57.22	58.01	56.62	62.27	63.69	64.29
TiO2	0.93	1.17	0.85	0.79	0.65	0.6
Al2O3	20.47	18.72	18.66	15.39	15.41	14.7
Fe tot	8.81	7.59	8.01	7.04	5.95	5.13
MnO	0	0.06	0.09	0.05	0.09	0.09
MgO	4.06	3.32	4.38	3.87	4.2	3.66
CaO	1.47	0.7	3.29	1.47	2.81	4.34
Na2O	3.94	3.43	2.5	3.94	3.08	3.17
K2O	3.67	2.16	3	3.67	2.24	1.96

MICROPROBE ANALYSES

PELITES

biotite

SiO2	35.08	36.24	35.35	38.10	32.90	34.22	43.58
TiO2	2.96	2.05	2.13	1.80	1.67	2.20	1.61
Al2O3	16.12	15.74	18.45	19.71	18.42	18.83	15.52
Fe2O3	0.48	0.00	0.00	0.00	6.84	0.00	0.00
FeO	19.09	18.98	20.85	19.00	16.65	21.29	19.25
MnO	0.20	0.18	0.00	0.00	0.00	0.00	0.00
MgO	11.76	11.64	8.79	7.81	10.07	8.65	7.64
CaO	0.05	0.01	0.04	0.49	0.04	0.02	0.05
Na2O	0.07	0.09	0.07	0.11	0.06	0.05	0.05
K2O	7.06	9.00	8.91	7.59	5.82	9.06	6.85
H2O	3.87	3.86	3.87	4.00	3.85	3.83	4.05
Total	96.72	97.79	98.45	98.61	96.31	98.14	98.60

no. of ions on the basis of 11 O

Si	2.72	2.81	2.74	2.86	2.56	2.68	3.23
Ti	0.17	0.12	0.12	0.10	0.10	0.13	0.09
Al	1.47	1.44	1.69	1.74	1.69	1.74	1.36
Fe3	0.03	0.00	0.00	0.00	0.40	0.00	0.00
Fe2	1.24	1.23	1.35	1.19	1.08	1.39	1.19
Mn	0.01	0.01	0.00	0.00	0.00	0.00	0.00
Mg	1.36	1.35	1.02	0.87	1.17	1.01	0.84
Ca	0.00	0.00	0.00	0.04	0.00	0.00	0.00
Na	0.01	0.01	0.01	0.02	0.01	0.01	0.01
K	0.70	0.89	0.88	0.73	0.58	0.90	0.65
H	2.00	2.00	2.00	2.00	2.00	2.00	2.00
total	9.71	9.87	9.81	9.55	9.59	9.87	9.37

white micas

SiO2	47.47	48.58
TiO2	0.67	0.68
Al2O3	34.50	36.92
Fe2O3	3.45	1.36
FeO	0.00	0.00
MnO	0.02	0.00
MgO	1.50	0.58
CaO	0.28	0.05
Na2O	0.56	0.40
K2O	8.59	9.94
H2O	4.67	4.72
Total	101.71	103.24

no. of ions on the basis of 11 O

Si	3.05	3.08
Ti	0.03	0.03
Al	2.61	2.76
Fe3	0.17	0.07
Fe2	0.00	0.00
Mn	0.00	0.00
Mg	0.14	0.05
Ca	0.02	0.00
Na	0.07	0.05
K	0.70	0.81
H	2.00	2.00
Total	8.79	8.86

chlorite

SiO2	26.57	31.18	26.06
TiO2	0.1	0.09	0.45
Al2O3	21.05	20.59	20.47
FeO	26.28	23.4	25.75
MnO	0	0	0
MgO	13.62	11.82	13.78
CaO	0.01	0.11	0.06
Na2O	0	1.56	0.01
K2O	0.15	0.21	0.14
H2O	11.37	11.66	11.23
Total	99.16	100.6	97.94

no. of ions on the basis of 18 O

Si	2.80	3.21	2.78
Ti	0.01	0.01	0.04
Al	1.41	1.71	1.36
Fe2	2.32	1.65	2.30
Mn	0.00	0.00	0.00
Mg	0.13	0.00	0.16
Ca	0.00	0.00	0.00
Na	0.00	0.01	0.01
K	0.02	0.77	0.85
H	8.00	8.00	8.00
total	14.69	15.36	15.50

feldspars

SiO2	62.93	66.60	64.11
TiO2	0.09	0.00	0.03
Al2O3	20.42	18.26	18.18
Fe2O3	0.00	0.00	0.00
FeO	0.73	0.06	0.14
MnO	0.00	0.00	0.00
MgO	0.10	0.00	0.05
CaO	0.69	0.00	0.01
Na2O	5.64	0.54	0.58
K2O	7.02	15.41	15.57
Total	97.61	100.87	98.66

no. of ions on the basis of 8 O

Si	2.90	3.06	3.00
Ti	0.00	0.00	0.00
Al	1.11	0.99	1.00
Fe3	0.00	0.00	0.00
Fe2	0.03	0.00	0.01
Mn	0.00	0.00	0.00
Mg	0.01	0.00	0.00
Ca	0.03	0.00	0.00
Na	0.50	0.05	0.05
K	0.41	0.90	0.93
Anorthit	0.04	0.00	0.00
Albite	0.53	0.05	0.05
Orthocl	0.43	0.95	0.95

SPOTTED SLATES

biotite

SiO2	41.99	37.57	31.54	28.66	38.70	32.44	32.75	32.85	34.71	32.18	34.61	37.27	33.56
TiO2	0.14	1.39	2.40	0.08	11.45	2.12	2.87	2.66	2.51	1.83	2.91	2.11	2.68
Al2O3	29.50	26.28	19.62	22.41	25.26	20.81	18.81	18.98	22.56	20.39	19.10	20.15	19.12
Fe2O3	0.00	0.00	6.94	29.53	0.00	3.01	0.00	0.00	0.00	6.41	0.00	0.00	0.20
FeO	9.61	14.62	16.33	4.51	9.92	18.57	21.12	21.65	18.51	18.82	23.69	20.83	23.78
MnO	0.07	0.04	0	0.03	0.00	0	0	0	0.14	0.14	0.17	0.11	0.12
MgO	4.75	6.29	9.45	8.02	4.36	8.29	8.49	8.33	7.33	8.94	8.21	6.98	8.34
CaO	0.01	0.03	0.08	0.04	0.08	0.06	0.04	0.09	0.14	0.03	0.04	0.02	0.02
Na2O	0.24	0.07	0.08	0.03	0.06	0.09	0.17	0.12	0.18	0.11	0.16	0.13	0.10
K2O	7.30	3.40	5.37	0.16	4.90	5.44	7.31	7.19	5.32	6.62	8.40	6.71	7.49
H2O	4.26	3.99	3.83	3.99	4.05	3.01	3.75	3.76	3.85	3.92	3.92	3.93	3.88
Total	97.86	93.69	95.64	97.47	98.80	94.64	95.31	95.63	95.25	99.38	101.22	98.24	99.30

no. of ions on the basis of 11 O

Si	2.96	2.82	2.47	2.15	2.86	2.55	2.62	2.62	2.70	2.46	2.65	2.85	2.59
Ti	0.01	0.08	0.14	0.00	0.64	0.13	0.17	0.16	0.15	0.11	0.17	0.12	0.16
Al	2.45	2.33	1.81	1.99	2.20	1.93	1.77	1.78	2.07	1.84	1.72	1.81	1.74
Fe3	0.00	0.00	0.41	1.67	0.00	0.18	0.00	0.00	0.00	0.37	0.00	0.00	0.01
Fe2	0.57	0.92	1.07	0.28	0.61	1.22	1.41	1.44	1.21	1.20	1.52	1.33	1.53
Mn	0.00	0.00	0	0.00	0.00	0	0	0	0.01	0.01	0.01	0.01	0.01
Mg	0.50	0.70	1.10	0.90	0.48	0.97	1.01	0.99	0.85	1.02	0.94	0.79	0.96
Ca	0.00	0.00	0.01	0.00	0.01	0.01	0.00	0.01	0.01	0.00	0.00	0.00	0.00
Na	0.03	0.01	0.01	0.00	0.01	0.01	0.03	0.02	0.03	0.02	0.02	0.02	0.02
K	0.66	0.33	0.54	0.02	0.46	0.55	0.75	0.73	0.53	0.65	0.82	0.65	0.74
H	2.00	2.00	2.00	2.00	2.00	2.00	2.00	2.00	2.00	2.00	2.00	2.00	2.00
total	9.17	9.19	9.55	9.02	9.28	9.55	9.77	9.75	9.55	9.66	9.85	9.59	9.75

white micas

SiO2	48.18
TiO2	0.01
Al2O3	35.87
Fe2O3	3.16
FeO	0.00
MnO	0.00
MgO	1.52
CaO	0.26
Na2O	0.15
K2O	4.80
H2O	4.75
Total	98.70

no. of ions on the basis of 11 O

Si	3.04
Ti	0.00
Al	2.67
Fe3	0.15
Fe2	0.00
Mn	0.00
Mg	0.14
Ca	0.02
Na	0.02
K	0.39
H	2.00
Total	8.42

pinite spots

SiO2	50.20	52.14	59.20	55.93	51.91	48.07	44.51	52.21	56.79
TiO2	0.06	0.10	0.22	0.19	0.02	0.76	2.34	0.66	0.19
Al2O3	32.75	28.21	24.22	25.97	32.12	25.84	23.51	27.13	28.93
Fe2O3	0.00	0.00	0.00	0.00	0.00	0.00	0.00	0.00	0.00
FeO	2.91	7.05	5.01	4.65	2.58	8.21	13.54	6.51	3.37
MnO	0.02	0.02	0.02	0.07	0.02	0.06	0.07	0.04	0.03
MgO	1.36	2.42	2.66	2.10	1.56	3.49	5.14	2.66	1.54
CaO	0.05	0.06	0.03	0.42	0.80	1.23	0.18	0.86	0.45
Na2O	0.15	0.13	0.17	0.79	1.16	2.17	0.30	1.61	0.71
K2O	8.98	6.34	6.05	4.93	4.09	4.94	5.37	4.46	4.36
total	96.48	96.46	97.58	95.04	94.25	94.77	94.95	96.14	96.35

HORNFELS																															
biotite																	white micas						chlorite								
SiO2	35,08	36,24	36,29	36,46	35,70	35,77	27,47	36,39	29,80	34,31	29,48	32,45	31,32	32,85	33,09		SiO2	49,89	47,88	45,37			SiO2	27,46	24,05	29,48						
TiO2	2,96	2,05	2,86	2,85	2,87	2,78	0,19	2,10	1,14	2,19	0,86	1,68	1,32	1,94	1,78		TiO2	0,14	0,03	0,68			TiO2	0,19	0,05	0,86						
Al2O3	16,12	15,74	15,45	15,38	15,75	15,98	19,34	16,32	19,20	18,77	18,70	19,72	19,27	19,02	18,81		Al2O3	32,27	31,14	30,55			Al2O3	19,34	18,34	18,7						
Fe2O3	0,48	0,00	0,00	0,00	0,00	0,00	24,10	0,00	22,55	0,00	16,76	7,53	13,13	3,69	5,31		Fe2O3	2,36	4,88	5,12			FeO	21,68	31,81	20,81						
FeO	19,09	18,98	19,26	18,74	19,28	19,72	0,00	19,14	2,42	20,07	5,73	13,78	10,85	17,53	15,80		FeO	0,00	0,00	0,00			MnO	0	0,23	0,22						
MnO	0,20	0,18	0,24	0,23	0,21	0,25	0	0	0,22	0,21	0,22	0,18	0,21	0,18	0,21		MnO	0,03	0,06	0,07			MgO	15,88	11,06	11,48						
MgO	11,76	11,64	11,42	11,40	11,44	11,75	15,88	12,43	13,14	9,86	11,48	11,11	10,84	10,03	10,75		MgO	1,83	3,32	3,42			CaO	0,05	0,17	0,47						
CaO	0,05	0,01	0,00	0,00	0,04	0,04	0,05	0,02	0,04	0,08	0,47	0,13	0,07	0,04	0,05		CaO	0,03	0,06	0,10			Na2O	0	0,04	0,35						
Na2O	0,07	0,09	0,08	0,08	0,08	0,06	0,00	0,07	0,04	0,19	0,35	0,11	0,07	0,07	0,07		Na2O	0,47	0,18	0,44			K2O	0,22	0,22	2,11						
K2O	7,06	9,00	8,91	9,20	8,08	7,43	0,22	8,16	3,22	7,46	2,11	5,51	4,48	6,25	5,96		K2O	8,19	8,76	7,11			H2O	11,24	10,64	11,15						
H2O	3,87	3,86	3,87	3,86	3,85	3,89	3,95	3,93	3,94	3,84	3,72	3,89	3,87	3,82	3,86		H2O	4,63	4,66	4,54			Total	96,06	96,61	95,63						
Total	96,72	97,79	98,37	98,20	97,31	97,68	91,20	98,56	95,72	96,98	89,88	96,07	95,42	95,44	95,68		Total	99,84	100,98	97,41												
																							no. of ions on the basis of 18 O									
no. of ions on the basis of 11 O																	no. of ions on the basis of 11 O														
																							Si	2,93	2,71	3,17						
Si	2,72	2,81	2,82	2,83	2,78	2,75	2,09	2,77	2,27	2,68	2,38	2,50	2,43	2,58	2,57		Si	3,23	3,08	2,99			Ti	0,01	0,00	0,07						
Ti	0,17	0,12	0,17	0,17	0,17	0,16	0,01	0,12	0,07	0,13	0,05	0,10	0,08	0,11	0,10		Ti	0,01	0,00	0,03			Al	2,04	2,44	2,37						
Al	1,47	1,44	1,41	1,41	1,45	1,45	1,73	1,47	1,72	1,73	1,78	1,79	1,76	1,76	1,72		Al	2,47	2,36	2,38			Fe2	1,93	3,00	1,87						
Fe3	0,03	0,00	0,00	0,00	0,00	0,00	1,38	0,00	1,29	0,00	1,02	0,44	0,77	0,22	0,31		Fe3	0,11	0,24	0,25			Mn	0,00	0,02	0,02						
Fe2	1,24	1,23	1,25	1,22	1,26	1,27	0,00	1,22	0,15	1,31	0,39	0,89	0,70	1,15	1,03		Fe2	0,00	0,00	0,00			Mg	2,52	1,86	1,84						
Mn	0,01	0,01	0,02	0,02	0,01	0,02	0	0	0,01	0,01	0,02	0,01	0,01	0,01	0,01		Mn	0,00	0,00	0,00			Ca	0,01	0,02	0,05						
Mg	1,36	1,35	1,32	1,32	1,33	1,35	1,80	1,41	1,49	1,15	1,38	1,28	1,25	1,17	1,25		Mg	0,18	0,32	0,34			Na	0,00	0,01	0,07						
Ca	0,00	0,00	0,00	0,00	0,00	0,00	0,00	0,00	0,00	0,01	0,04	0,01	0,01	0,00	0,00		Ca	0,00	0,00	0,01			K	0,03	0,03	0,29						
Na	0,01	0,01	0,01	0,01	0,01	0,01	0,00	0,01	0,01	0,03	0,06	0,02	0,01	0,01	0,01		Na	0,06	0,02	0,06			H	8,00	8,00	8,00						
K	0,70	0,89	0,88	0,91	0,80	0,73	0,02	0,79	0,31	0,74	0,22	0,54	0,44	0,63	0,59		K	0,68	0,72	0,60			total	17,47	18,09	17,76						
H	2,00	2,00	2,00	2,00	2,00	2,00	2,00	2,00	2,00	2,00	2,00	2,00	2,00	2,00	2,00		H	2,00	2,00	2,00												
total	9,71	9,87	9,87	9,89	9,81	9,74	9,03	9,80	9,32	9,78	9,31	9,57	9,46	9,64	9,61		Total	8,74	8,75	8,66												
feldspars																															
										no. of ions on the basis of 8 O																					
SiO2	45,62	61,26	84,89	66,46	62,28	66,22	68,12	66,62																							
TiO2	0,04	0,00	0,03	0,02	0,00	0,00	0,02	0,00		Si	2,52	2,75	4,61	2,95	2,75	2,90	2,93	2,96		Anorthit	0,27	0,25	0,12	0,22	0,30	0,16	0,09	0,16	
Al2O3	22,40	24,31	4,98	22,66	24,23	22,15	20,79	21,02		Ti	0,00	0,00	0,00	0,00	0,00	0,00	0,00	0,00		Albite	0,72	0,74	0,09	0,77	0,69	0,84	0,90	0,84	
Fe2O3	0,17	0,00	0,00	0,00	0,00	0,00	0,00	0,00		Al	1,46	1,29	0,32	1,19	1,26	1,14	1,06	1,10		Orthoclt	0,02	0,01	0,80	0,01	0,01	0,01	0,00	0,01	
FeO	0,00	0,07	0,67	0,15	0,17	0,14	0,23	0,25		Fe3	0,01	0,00	0,00	0,00	0,00	0,00	0,00	0,00											
MnO	0,02	0,04	0,04	0,02	0,00	0,01	0,00	0,01		Fe2	0,00	0,00	0,03	0,01	0,01	0,00	0,01	0,01											
MgO	0,05	0,02	0,25	0,00	0,00	0,01	0,02	0,01		Mn	0,00	0,00	0,00	0,00	0,00	0,00	0,00	0,00											
CaO	4,56	4,93	0,04	3,99	6,18	3,21	2,01	3,09		Mg	0,00	0,00	0,02	0,00	0,00	0,00	0,00	0,00											
Na2O	6,73	8,05	0,02	7,65	7,95	9,34	10,84	9,10		Ca	0,27	0,24	0,00	0,19	0,29	0,15	0,09	0,15											
K2O	0,26	0,22	0,23	0,12	0,15	0,08	0,06	0,10		Na	0,72	0,70	0,00	0,66	0,68	0,79	0,91	0,78											
Total	79,84	98,90	91,15	101,08	100,96	101,17	102,08	100,21		K	0,02	0,01	0,02	0,01	0,01	0,00	0,00	0,01											